Analysis of High-Speed Train Braking Systems: Components, Braking Force, and Air Consumption

P. Paryanto[a,*], Joga D. Setiawan[a], Abduh B. Adriathma[a], Akhmat Busori[b], Mulyadi S. Harjono[c], Nur Cahyo[d]

[a] Department of Mechanical Engineering, Diponegoro University
Jl. Prof Soedarto, SH, Tembalang, Semarang, Indonesia
[b] R&D Department, PT. Industri Kereta Api (INKA)
Jl. Yos Sudarto No 71, Madiun, Indonesia
[c] National Research and Innovation Agency (BRIN)
Jl. M.H. Thamrin No.8, Jakarta, Indonesia
[d] PLN Research Institute
Jl. Duren Tiga Raya No.102, Jakarta, Indonesia
*E-mail: paryanto@ft.undip.ac.id

Abstract

Ensuring the accuracy of parameters involved in high-speed train braking is essential for passenger safety and efficient operation. To achieve this, it is crucial to verify the force values, input and output specifications of braking system devices, and ensure they align with the desired values. This can be accomplished through quantitative research, which involves collecting braking system data from the train manufacturing company and consulting the technical book provided by the braking system manufacturer. In this particular research, the braking system of the high-speed train under investigation is designed as a combination of regenerative and electro-pneumatic braking. The regenerative braking force, determined by the DC motor and control, amounts to 95.46 kN, enabling train to decelerate from 220 km/h to 90 km/h. Subsequently, the electro-pneumatic braking continues the regenerative braking, with a force value resulting from the calculation of the output value on devices of 296.4 kN, bringing train to a complete stop. The air demand required to supply the pneumatic components of braking devices as well as the air demand of other devices in train is 121.35 liters/min. This figure accounts for the pneumatic supply needed for braking system's proper functioning, along with other pneumatic-dependent devices present on train. To validate the proposed design, a simulation of train braking operations was conducted using the data obtained from the research. This simulation aims to evaluate the effectiveness and efficiency of high-speed train braking system design, providing valuable insights for further improvements and optimizations.

Keywords: braking system devices; high-speed train; hybrid train

Abstrak

Keakuratan parameter pada pengereman kereta cepat menjadi faktor penting dalam operasional dan keselamatan penumpang. Nilai gaya dan spesifikasi input serta output perangkat sistem pengereman perlu untuk dipastikan, sehingga memiliki nilai yang tepat dan sesuai dengan yang diinginkan. Menggunakaan penelitian kuantitatif dengan pengambilan data sistem pengereman di perusahaan manufaktur kereta, serta menggunakan buku teknis perusahaan produsen sistem pengereman memberikan hasil desain sistem pengereman yang dapat diterapkan. Sistem pengereman kereta cepat penelitian ini merupakan kombinasi pengereman regeneratif dan elektro-pneumatik. Gaya pengereman regeneratif sebesar 95,46 kN ditentukan oleh motor DC serta kontrol memberikan perlambatan kereta dari kecepatan 220 km/h menjadi 90 km/h. Pengereman elektro-pneumatik melanjutkan pengereman regeneratif, dengan nilai gaya hasil dari perhitungan nilai output pada perangkat, sebesar 296,4 kN untuk memberhentikan kereta. Kebutuhan udara yang diperlukan untuk memberikan suplai terhadap komponen pneumatik perangkat pengereman serta kebutuhan udara perangkat lainnya dari kereta yaitu sebesar 121,35 liter/min. Hasil dari penelitian ini dipakai untuk menjalankan simulasi operasional pengereman kereta, sehingga desain sistem pengereman kereta cepat dapat ditentukan.

Kata kunci: kereta cepat; kereta hybrid; perangkat sistem pengereman

1. Introduction

Braking a high-speed train poses significant challenges due to the need to effectively slow down and bring the train to a complete stop while it is traveling at exceptionally high speeds [1]. Braking system of high-speed train encompasses a complex multi-components process involving a combination of mechanical, pneumatic, hydraulic, and electronic devices [2]. The selection of the braking type is influenced by various factors, including the train's situation, conditions, and both internal and external factors. The parameter values of the braking system are crucial as they have a significant impact on the accuracy and success of the braking process. Ensuring the accuracy of these parameter values is vital for ensuring the safety and security of the passengers on board.

To address these challenges, this research aims to identify the technical components of the high-speed train braking system, specifically focusing on the combined system of regenerative and electro-pneumatic devices. The research also involves calculating the braking force and air demand, as well as obtaining a comprehensive list of the main devices in the high-speed train braking system. These results serve as input values for modeling and simulating the longitudinal dynamics of the train during high-speed braking. It is important to note that, the discussion of high-speed train braking system is designed for train that have three car bodies, operating on a flat straight line with no gradient or curve curvature, and operating in service braking.

2. Materials and Methods

The calculation of braking force is essential as it provides the value based on braking device specifications and the required braking conditions, taking into account performance tolerances [3]. This calculation serves as a basis for determining braking parameters. Furthermore, the list of main devices supports the identification of the processing circuit during braking, facilitating the understanding of system requirements for manufacturing and assembly purposes. The use of air consumption is calculated to determine the specifications of air supply and storage devices that are suitable for the needs. In determining the compressor specification, the relative duty cycle parameter must be above the calculated requirement, including the charging time [4].

In this research, the scientific data were obtained from collaborative research between universities and institutions in Indonesia as well as data collection at train manufacturing companies. The equations for calculating braking force and air consumption were obtained from the technical book by braking company Knoor-Bremse and the handbook of railway vehicle dynamics [5]. Train specification data, shown in Table 1, were obtained from field data and calculations by an Indonesian train manufacturing company. Then, the results of these calculations become parameters in the design of components and system.

Table 1
Train specification data

General Specifications		
a	Type	Hybrid (diesel engine and battery)
b	Carriage configuration	MEC + T + MEC
c	Engine	On floor 2 x 500 kW (continuous rated)
d	Train weight	The static mass is 168 tons with an axle mass of 14 tons.
e	Passenger capacity	32 passengers per MEC carriage. 90 passengers per T carriage.
f	Design speed	220 km/h
Propulsion System		
g	Voltage	600 VDC
h	Power	@ 315 kW total of 8 set
i	Voltage converter	PWM Rectifier
j	Battery capacity	850 kWh, C-Rate min 2C

3. Result and Discussion

3.1 Regenerative Braking Force

Regenerative braking uses a traction motor converted into a generator [6]. In system modeling, regenerative braking is performed at a distance of 3 km with a change in speed from 220 km/h to 90 km/h, while the mass of the moving train is 194.2 tons, consisting of static and dynamic masses. Braking scheme of train is shown in Fig.1.

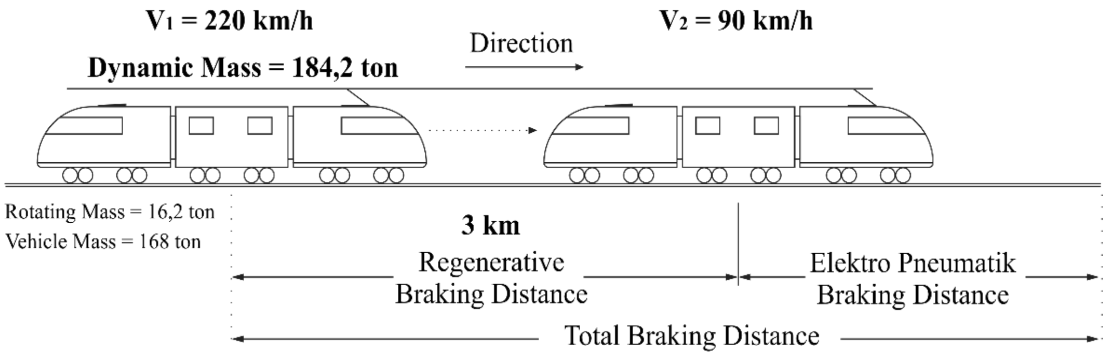

Fig. 1 Braking schematic

The value of the regenerative braking force at a given distance can be found in Equation 1, which relates kinetic energy and braking force. The regenerative braking force was applied to train at speed of 220 km/h in a way that train decelerates to speed of 90 km/h with a force of 95.46 kN. The regenerative braking force value is affected by the DC motor and its control.

$$F_{Rem\_Reg} = \frac{EK_{Reg}}{s_{Reg}} \tag{1}$$

DC Motor

The DC motor is the main components of regenerative braking, this device acts as a generator. During braking, an electric current flows through the DC motor to generate a magnetic field in the stator [7]. This magnetic field then slows down the rotation of the rotor, causing train wheels to slow down. The sub-components of a DC motor are the coil, commutator, rotor, and stator [8]. The schematic of the DC motor traction devices is shown in Fig. 2.

Coil

The coil produces a magnetic field that rotates the rotor, and the number of turns affects the generated magnetic field, the more turns, the stronger the magnetic field produced [9]. When the magnetic field is generated, a back EMF is generated due to the deceleration of rotation in the rotor. This back EMF is used to charge the energy in the storage system.

Commutator

The commutator rotates the electric current in the DC motor when the rotor rotates. When electric current flows into the motor and through the commutator, it produces a negative torque that slows [10] or stops the movement of the DC motor.

Rotor

The rotor is the part rotating and carries the load or charge, which consists of a series of wire windings attached to the shaft. Increasing the number of turns increases the strength of the magnetic field in the rotor and produces greater torque, but this also results in greater electrical resistance, which reduces the efficiency of the motor [11]. The number of turns also affects the rotor inertia and response time of the motor, the more wire turns, the greater the rotor inertia and the slower the response time.

Stator

The stator becomes a static part and influences the characteristics of the motor, namely the formation of the magnetic field due to the wire coils in the stator and the determination of the torque generated on the rotor [12].

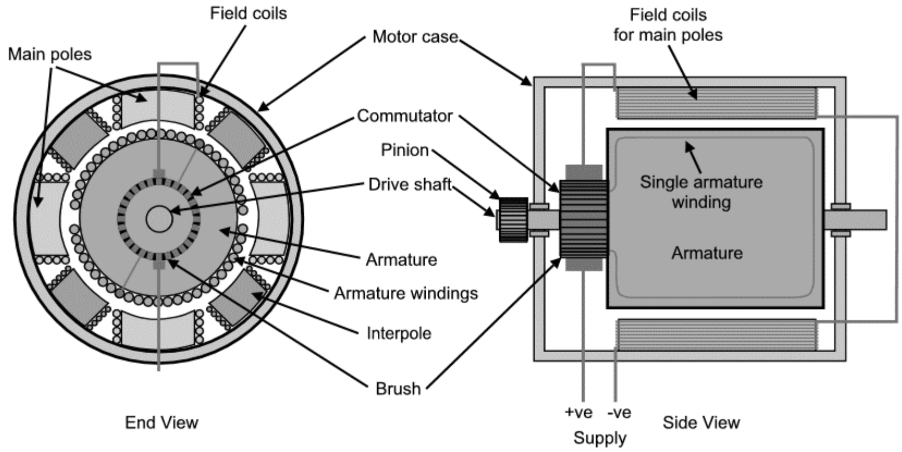

Fig. 2 DC motor devices (http://www.railway-technical.com)

Control System and Motor Controller

The control system is used to control the operation of the DC motor, including when it functions as a generator. While the motor controller regulates speed and direction of rotation of the DC motor [13], the function of the DC motor changes from a motor to a generator and produces negative torque used to slow down train.

The working efficiency of system is affected by the torque control technology used, and one of these technologies is the direct torque control (DTC) technique. DTC is a motor control method that provides precise torque control and is responsive to application needs [14]. This control utilizes the direct measurement of the DC motor's back EMF to control the motor's current and torque.

3.2 Electro-Pneumatic Braking Force

Combining the Different Brake System

The calculation of the parameter combining the different brake system shows the value of the total force acting on braking system of each carriage. The electro-pneumatic braking sub-system applied to each carriage is not always the same. On trailer vehicles, only a friction braking system is used, while on vehicles with passenger cars, a mixed braking system is used, namely braking performed by motor dynamics combined with friction brake braking. The force value of combining the different brake system is shown in Eq. 2.

$$F_{Rem\_P} = F_{B\_i\_MEC} + F_{B\_i\_T} + F_{B\_i\_MEC} \tag{2a}$$

$$F_{B\_i\_MEC} = \left(F_{BED} \times \Sigma\left(n_{axle\_BED\_MEC}\right)\right) + \left(F_{BEP} \times \Sigma\left(n_{axle\_BEP\_MEC}\right)\right) \tag{2b}$$

$$F_{B\_i\_T} = F_{BEP} \times \Sigma\left(n_{axle\_BEP\_T}\right) \tag{2c}$$

The value is dependent on the number of axles installed, and each train bogie consists of 2 or 3 axles, as shown in Fig. 3. On each axle, 2 caliper units on each side function to provide friction against the brake pad, and hence, the wheel rotation can slow down.

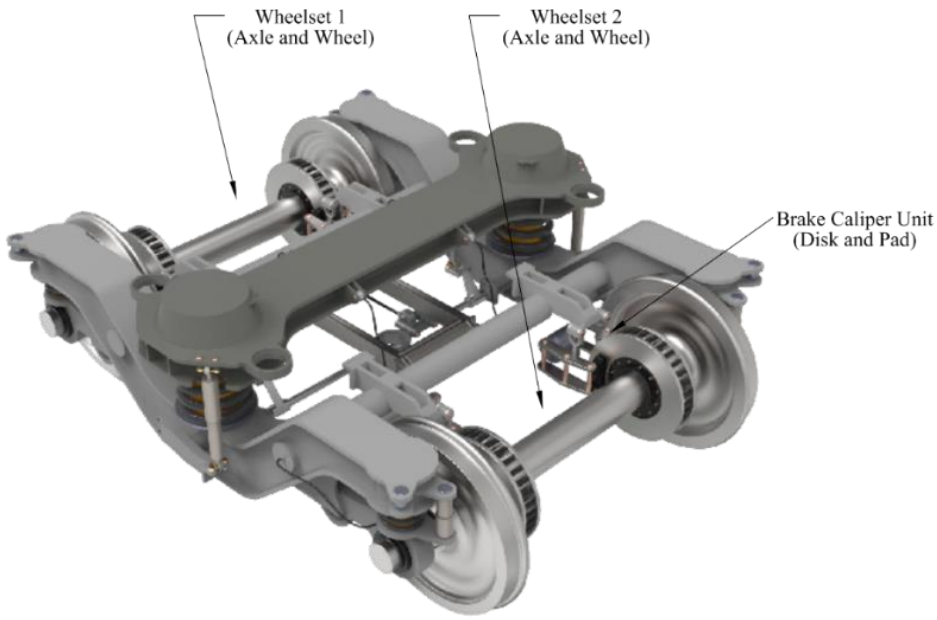

Fig. 3 Train bogies with 2 axles (https://grabcad.com/library/lhb-fiat-bogie-1)

Mean Electrodynamic Braking Force

The average electrodynamic braking force calculation is the value of the dynamic engine braking force [7] which is only carried out on the axle containing the motor in a way that it only occurs on the motor car. The value of the mean electrodynamic braking force is influenced by the initial speed per motor on the axle, as for the sub-components of the motor devices shown in Fig. 2.

Braking Force per Axle (Based on Wheel Diameter)

The calculation of this parameter is the value of braking force generated on each axle from the friction occurring in the brake caliper unit, namely between the brake disc and brake pad, as shown in Fig. 4. This value is influenced by the mean friction coefficient of the brake pad, the number of brake discs per disc, the mean swept radius, the wheel diameter, the transmission ratio, and the transmission efficiency.

The mean friction coefficient of a brake pad has values based on brake pad material, speed, temperature, and braking time. Higher speed, the lower the value of the brake pad coefficient. The surface pressure is related to the roughness of the surface in direct contact with the brake disc. The temperature will increase as braking force increases, and the increase in temperature will reduce the coefficient of friction of the brake pad. The longer braking time, the greater the value of the brake pad coefficient. Braking needs to pay attention to the non-slip state of the rail track, and hence, the coefficient of friction of the brake pad with the brake disc should be smaller than the coefficient of friction of the wheel with the rail [8]. The mean value of the friction coefficient of the brake pad applied to this system is 0.35. The number of brake discs installed per axle is 2, as shown in Fig. 5.

The mean swept radius of the wheel is the average distance from the wheel center to the disc surface [15]. The mean swept radius affects braking efficiency, the larger the mean swept radius value, the greater braking force generated, which allows train to stop faster. However, a value that is too high can impair driving comfort and, due to increased stress on the wheel bearings, shorten the service life of the brake pads. The mean swept radius value used in high-speed train is 251 mm.

The diameter of the wheels takes into account several factors, such as vehicle weight, maximum vehicle speed, and route characteristics. A wheel diameter value that is too small results in insufficient braking force to slow or stop train effectively, but a wheel diameter that is too large results in excessive braking force. The diameter value of the wheel on high-speed train is 920 mm.

The transmission ratio is the ratio between the rotation speed of the motor shaft and the rotation speed of the brake disc. With a service brake, braking system uses a gear with a low transmission. However, a transmission ratio that is too low can reduce the brake disc rotation speed and reduce braking effectiveness, while a transmission ratio that is too high increases the brake disc rotation speed and causes the brake disc to overheat. The transmission ratio value used in the service brake system of high-speed train is 1.

Transmission efficiency is the efficiency of power transmission from the electric motor to braking system in the brake caliper unit. Some factors that affect transmission efficiency are the quality of the gearbox and clutch, the match between the electric motor and braking system, and the efficiency of energy conversion from electrical to mechanical (16). The assumed value of transmission efficiency in this system is 100%.

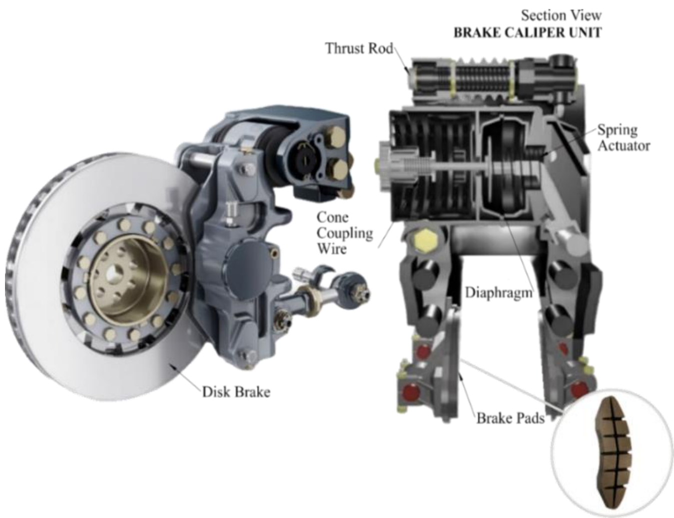

Fig. 4 Brake caliper unit devices (https://howtechnologyworks3d.com)

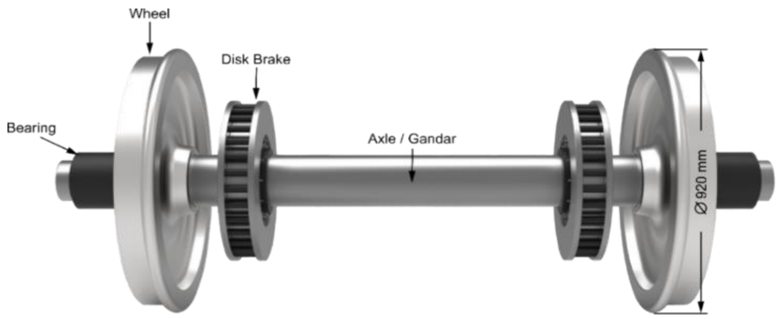

Fig. 5 Axle components on train bogies (https://grabcad.com/library/lhb-fiat-bogie-1)

Total Force on The Brake Pad per Disk

The calculation of the total force on the brake pad per disc is the value of braking force generated on the brake caliper unit, while this value is influenced by brake cylinder pressure, force pressure ratio, and additive value.

The brake cylinder pressure can be seen in Fig.8 with a value of 3.8 bar. The pressure value in the brake cylinder pressure is obtained from the initial value of the air volume in the reservoir, as shown in Fig. 6, where the air volume in the tank is 75 liters. Then the value of brake cylinder pressure is also influenced by the final volume value [16], which is a volume consisting of a reservoir volume of 75 liters, a brake pipe with a volume of 70.9 liters, and a connecting brake pipe with a volume of 0.45 liters (shown in Fig. 7), and a brake cylinder (shown in Fig. 8) volume of 15.5 liters.

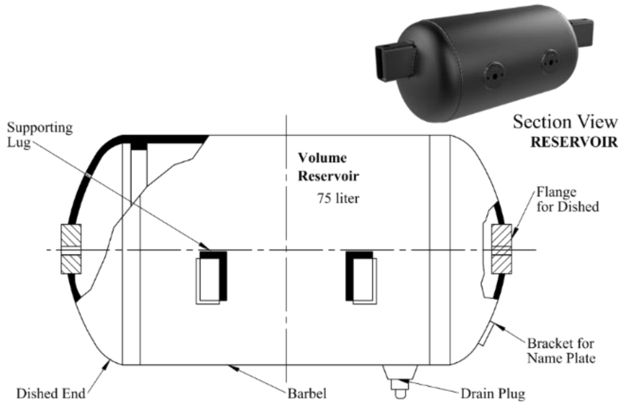

Fig. 6 Train reservoir equipment

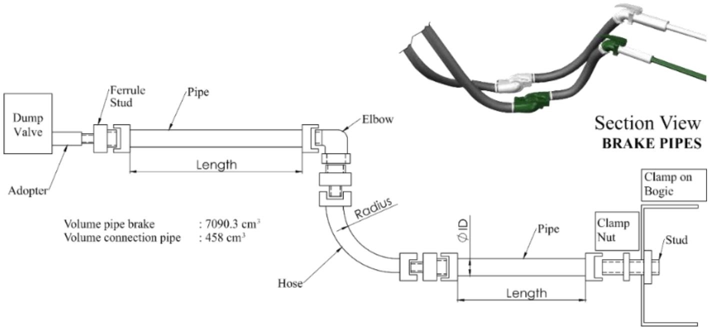

Fig. 7 Brake pipes devices

The force pressure ratio in electro-pneumatic braking applied to this system is 9.2 kN/bar. The force pressure ratio value is influenced by the brake cylinder piston area shown in Fig. 8 with a value of 510.7 cm2, the internal brake cylinder ratio with a value of 1, the rigging ratio with a value of 1.9, and the rigging efficiency with a value of 0.95. Then, the additive value that affects the value of the electro-pneumatic braking force of this system is -2707.5 N, since the value obtained from the internal brake cylinder force on the brake cylinder is -1500, the rigging ratio is 1.9, and the rigging efficiency is 0.95.

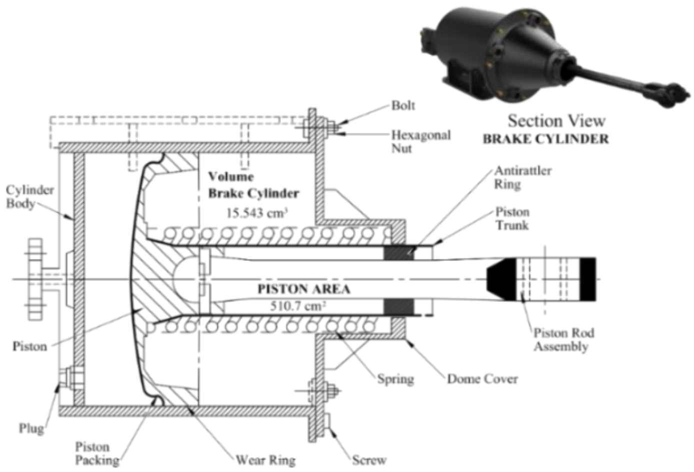

Fig. 8 Brake cylinder devices

The results of the parameter calculations for the components and sub-components of the electro-pneumatic braking devices can be seen in Table 2. The final value of the electro-pneumatic braking force acting on the 3 cars of high-speed train series based on Equation 2, is 296.4 kN.

Table 2
Electro-pneumatic braking calculation parameters

No	E-P Parameter Calculation	Value	Unit
A	**Service Brake with Blending Brake**		
1	Combining the different brake system (blending)	98.8	kN
2	Mean electrodynamic braking force depends on the initial speed	12.35	kN
3	Braking force per axle (based on wheel diameter)	12.35	kN
4	The total force on the brake pad per disk	32.32	kN
5	Brake cylinder Pressure	3.8	kg/cm^2
6	Pressure ratio	921.8135	kN/bar
7	Additive value	2,707.5	N
B	**Service Brake with Friction Brake Only**		
1	Combining the different brake system (single)	98.8	kN
2	Braking force per axle (based on wheel diameter)	12.35	kN
3	The total force on the brake pad per disc	32.3214	kN
4	Brake cylinder pressure	3.8	kg/cm^2
5	Pressure ratio	921.8135	kN/bar
6	Additive value	-2,707.5	N

3.3 Braking Devices

In this research, braking devices of high-speed train are shown in Fig. 9. The figure shows the side view schematic of braking devices. As for the list of high-speed train braking devices, both regenerative braking and electro-pneumatic braking are shown in Table 3.

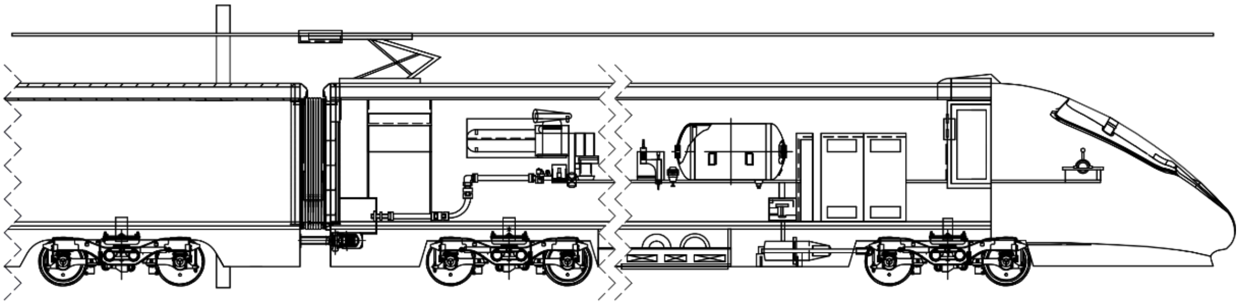

Fig. 9 Braking devices scheme on high-speed train

Table 3
Regenerative and electro-pneumatic braking devices

Regenerative Braking Devices	Electro-Pneumatic Braking Devices
3-phase induction motor	Driver's brake valve
Engine control unit	Compressor and auxiliary compressor
Energy storage system	Reservoir and auxiliary reservoir
Axle brush	Brake pipe
Transformer	Distributor valve
Inverter	Brake cylinder
Transmission system	Slack adjuster
Overhead single cable	Air dryer
Pantograph	Relay valve
	Pressure limiting valve
	Overflow valve
	Horn magnet valve
	Piston valve
	Two-way valve
	Pressure-reducing valve
	Oil separator
	Anti-skid valve
	Brake caliper unit

However, the list shows the main braking devices, while more details about the BOM of high-speed train braking devices cannot be presented because they require further review for application and assembly. Devices that were not included are the safety valve, screw plug, counter connector, sealing ring, stopcock, pressure sensor, check valve, pressure converter, pressure switch, test fitting, ballcock, bush, and so on.

3.4 Air Consumption

The use of air consumption determines the specifications of air supply and storage devices, which are compressors and reservoirs suitable for the needs. The relative duty cycle must be above the calculated requirements, including the charging time. The air consumption flow rate for each device on train is shown in Table 3, obtained from Eq. 3-8.

Brake cylinder

$$Q_{BrC\_Veh} = V_{BrC\_veh\_SB} \times \left(1 + \frac{k_{BR\_add}}{100}\right)\left(\frac{N_S}{60}\right) \tag{3}$$

Brake cylinder pipes

$$Q_{BrCP\_Veh} = V_{BrCP\_veh\_SB} \times \left(1 + \frac{k_{BR\_add}}{100}\right)\left(\frac{N_S}{60}\right) \tag{4}$$

Air suspension

$$Q_{AS\_s\_veh} = V_{AS\_s\_max\_veh} \times \left(\frac{k_{AS}}{100}\right)\left(\frac{N_S}{60}\right) \tag{5}$$

Door actuation

$$Q_{DO\_veh} = V_{DO\_veh} \times \left(\frac{k_{DO}}{100}\right)\left(\frac{N_S}{60}\right) \tag{6}$$

Whistle

$$Q_{HO\_veh} = V_{HO\_veh} \times \left(\frac{k_{HO}}{100}\right)\left(\frac{N_S}{60}\right) \tag{7}$$

Leakage

$$Q_{leak\_veh} = V_{tot\_veh} \frac{\left(\frac{q_{leak}}{3}\right)}{p_0} \tag{8}$$

Table 4
Volume and flow rate of air consumption

No	Air Consumption	Volume	Flow Rate
	Braking Devices		
1	Brake cylinder	19.33 liter	7.69 liter/min
2	Brake cylinder pipes	22.47 liter	8.94 liter/min
	Additional Devices		
3	Air suspension, static	2.028 liter	58.67 liter/min
4	Air suspension, dynamic	-	-
5	Door Actuation	75.6 liter	13.67 liter/min
6	Whistle	24 liter	4.34 liter/min
7	Leakage	841.2 liter	28.04 liter/min

The air consumption of high-speed train braking devices is influenced by braking specification and operational parameters, which are shown in Table 5.

Table 5
Air consumption parameter for braking devices

No	Parameter	Value
1	Car scheme	MEC + T + MEC
2	Number of brake cylinders per car	8-unit brake cylinder
3	Cylinder pressure for service brake operation	3,8 bar
4	Working volume of the brake cylinder for service brake	0,11 liter
5	Dead volume per cylinder brake	0,12 liter
6	Effective piston area	1,32 dm^2
7	Working stroke of the cylinder at service brake pressure	0,11 liter
8	Assumed length of brake cylinder pipes per car	21,6 meter
9	Free air pressure	1 bar
10	Additional brake actuation factor	10 %
11	Total number of stations	21
12	Driving time from the first to the last station	58 min

Based on the air consumption calculation, the required specification is a compressor with a flow rate of 121.35 liters/min. One of the air supply units capable of meeting the specified air demand is the VV120T compressor unit, which has a net air delivery of 656 liters/min and a relative duty cycle of 61.9%. One of the air supply units capable of meeting the specified air demand is the VV120T compressor unit. This particular unit has a net air delivery of 656 liters/min and a relative duty cycle of 61.9%.

4. Conclusion

In this research on high-speed train braking, we have successfully identified the braking system components, including braking force, a list of main devices, and air consumption. These findings are significant and have implications for further research, particularly in simulating the longitudinal dynamics of the train. The braking system of a high-speed train involves a combination of mechanical, pneumatic, and electronic devices, working together to achieve the necessary deceleration. By calculating the braking force of the high-speed train with a combined regenerative and electro-pneumatic braking system, we gain insights into the contribution of each sub-component of the braking devices to the overall parameter values. The regenerative braking system provides a force of 95.46 kN, while the electro-pneumatic braking system provides a force of 296.4 kN. Furthermore, we have determined that the air consumption of the braking system and other devices in the high-speed train requires a supply with a flow rate of 121.35 liters/min.

Acknowledgments

The authors are grateful to the National Research and Innovation Agency (BRIN) and The Indonesia Endowment Funds for Education (LPDP) at the Ministry of Finance for the Research and Innovation funding program “Riset dan Inovasi untuk Indonesia Maju” No 33/IV/KS/06/2022 and No 505/UN7.D2/KS/VI/2022, as well as PT. INKA, who provided research data making this important research feasible and effective.

References

[1] Wei L, Zeng J, Qu S, Huang C, Wang Q. Longitudinal-vertical dynamics of a high-speed train rescued by locomotives during braking on grades. Vehicle System Dynamics. 2022 Jun 3:1-24.
[2] Günay M, Korkmaz ME, Özmen R. An investigation on braking systems used in railway vehicles. Engineering Science and Technology, an International Journal. 2020 Apr 1;23(2):421-31.
[3] Zhao W, Ding J, Zhang Q, Liu W. Investigation into the braking performance of high-speed trains in the complex braking environment of the Sichuan-Tibet Railway. Proceedings of the Institution of Mechanical Engineers, Part F: Journal of Rail and Rapid Transit. 2022 Aug;236(7):766-82.
[4] Knoor-Bremse. Basics of brake technology [Internet]. 2022 [cited 2022 Apr 15]
[5] Iwnicki S. Handbook of railway vehicle dynamics. CRC press; 2006 May 22.
[6] Pavlović T, Župan I, Šunde V, Ban Ž. HIL simulation of a tram regenerative braking system. Electronics. 2021 Jun 9;10(12):1379.
[7] Tummuru NR, Misra H. Power management of Hybrid Energy Storage System based Wireless Charging system with Regenerative Braking capability. IEEE Transactions on Industry Applications. 2023 Jan 5.
[8] Abraham PK, Namboodiry J, Mary D. Experimental Validation of a Constant Torque Variable Deceleration Regenerative Braking System for a Brushless DC Motor. In2022 2nd International Conference on Power Electronics & IoT Applications in Renewable Energy and its Control (PARC) 2022 Jan 21 (pp. 1-6). IEEE.
[9] Das S. Modeling DC Motors and Their Control. In Modeling for Hybrid and Electric Vehicles Using Simscape 2022 Feb 12 (pp. 47-71). Cham: Springer International Publishing.
[10] Zhou Q, Shu J, Cai Z, Han C, Zhang Y. Optimal Duty Cycle Method to Suppress the Commutation Torque Ripple of Brushless DC Motor in Braking Mode. Journal of Electrical Engineering & Technology. 2022 May;17:1731-9.
[11] Saha B, Singh B. An Improved Flux Observer Based Position Sensorless Single Stage BLDC Motor Drive With Regenerative Braking For Solar Powered LEV. In2022 IEEE Transportation Electrification Conference & Expo (ITEC) 2022 Jun 15 (pp. 1248-1253). IEEE.
[12] Owatchaiphong S, Thumputi N. Dual Stator Winding Induction Motor in Regenerative Braking Operation of Electric Vehicles. In2022 25th International Conference on Electrical Machines and Systems (ICEMS) 2022 Nov 29 (pp. 1-5). IEEE.
[13] Roh C, Kwak S, Choi S. Three-phase three-level four-leg NPC converters with advanced model predictive control. Journal of Power Electronics. 2021 Oct;21:1574-84.
[14] Saiteja P, Ashok B, Wagh AS, Farrag ME. Critical review on optimal regenerative braking control system architecture, calibration parameters and development challenges for EVs. International Journal of Energy Research. 2022 Nov;46(14):20146-79.
[15] Varazhun I, Shimanovsky A, Zavarotny A. Determination of longitudinal forces in the cars automatic couplers at train electrodynamic braking. Procedia Engineering. 2016 Jan 1;134:415-21.
[16] Lu C, Wang Q, Wang Z, Mo J, Zhu S, Jin W.Stick–Slip Characteristic Analysis of High-Speed Train Brake Systems: A Disc–Block Friction System with Different Friction Radii. Vehicles. 2023 Jan 2;5(1):41-54.